



3 4456 0551022 0

ORNL/TM-6169

dy.1

Development of a Pneumatic Transfer System for HTGR Recycle Fuel Particles

J. E. Mack
D. R. Johnson

OAK RIDGE NATIONAL LABORATORY
CENTRAL RESEARCH LIBRARY
DOCUMENT COLLECTION

LIBRARY LOAN COPY

DO NOT TRANSFER TO ANOTHER PERSON

If you wish someone else to see this
document, send in name with document
and the library will arrange a loan.

UCN-7964
13 3-67

OAK RIDGE NATIONAL LABORATORY
OPERATED BY UNION CARBIDE CORPORATION · FOR THE DEPARTMENT OF ENERGY

ORNL/TM-6169
Distribution
Category UC-77

Contract No. W-7405-eng-26

METALS AND CERAMICS DIVISION

Thorium Utilization Program (189a OH045)

Fuel Refabrication — Task 500

DEVELOPMENT OF A PNEUMATIC TRANSFER SYSTEM
FOR HTGR RECYCLE FUEL PARTICLES

J. E. Mack and D. R. Johnson

Date Published: February 1978

NOTICE This document contains information of a preliminary nature.
It is subject to revision or correction and therefore does not represent a
final report.

OAK RIDGE NATIONAL LABORATORY
Oak Ridge, Tennessee 37830
operated by
UNION CARBIDE CORPORATION
for the
DEPARTMENT OF ENERGY

OAK RIDGE NATIONAL LABORATORY LIBRARIES



3 4456 0551022 0

CONTENTS

ABSTRACT	1
INTRODUCTION	1
TEST LOOP DESIGN	7
TRANSFER CHARACTERISTICS	10
PRODUCT INTEGRITY	17
APPLICATION TO ENGINEERING-SCALE EQUIPMENT	21
SUMMARY	21
ACKNOWLEDGMENTS	22
REFERENCES	22
APPENDIX A — PRESSURE DROP VS AIR VELOCITY IN HORIZONTAL AND VERTICAL CONVEYING	27
APPENDIX B — RESIN CARBONIZATION FURNACE PNEUMATIC TRANSFER SYSTEM	33

DEVELOPMENT OF A PNEUMATIC TRANSFER SYSTEM
FOR HTGR RECYCLE FUEL PARTICLES

J. E. Mack and D. R. Johnson

ABSTRACT

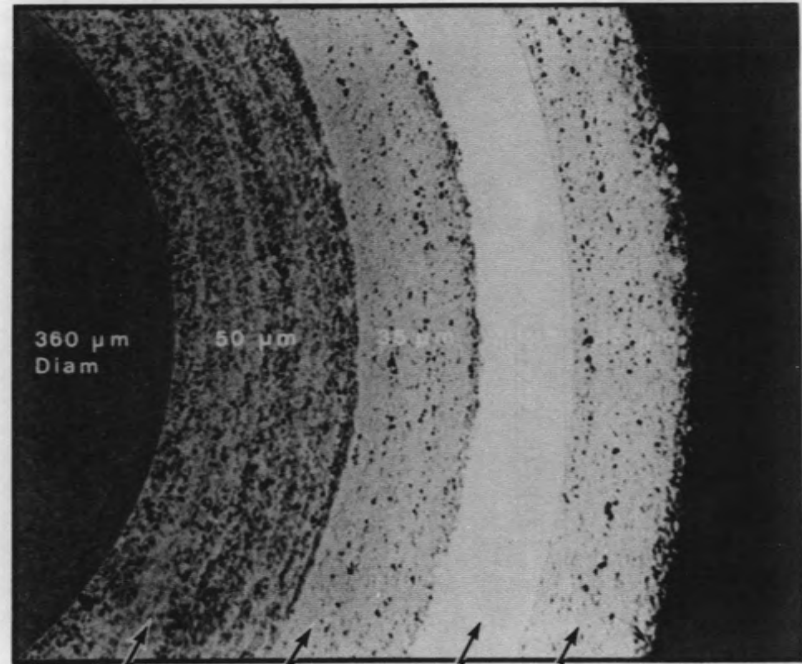
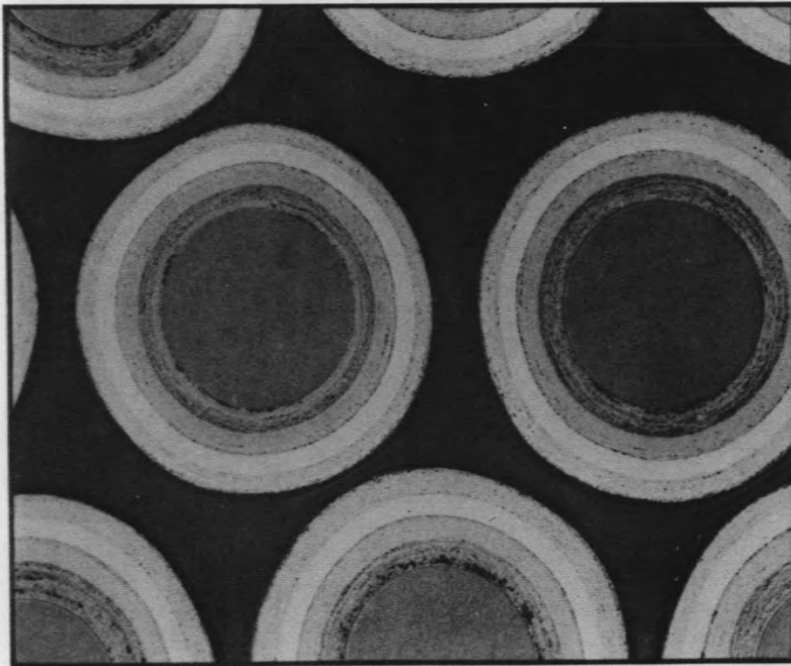
In support of the High-Temperature Gas-Cooled Reactor (HTGR) Fuel Refabrication Development Program, an experimental pneumatic transfer system was constructed to determine the feasibility of pneumatically conveying pyrocarbon-coated fuel particles of Triso and Biso designs. Tests were conducted with these particles in each of their nonpyrophoric forms to determine pressure drops, particle velocities, and gas flow requirements during pneumatic transfer as well as to evaluate particle wear and breakage. The results of this study indicated that the material can be pneumatically conveyed at low pressures without excessive damage to the particles or their coatings.

INTRODUCTION

Fabrication of HTGR recycle fuel elements must be performed in a remote facility due to the radiation hazard inherent to the recycle of ^{232}U -contaminated ^{233}U .¹ Pneumatic conveying possesses a number of distinct advantages over other types of material transfer for remote applications. The probability of equipment failure is very low since the transfer "mechanism" is compressed air or argon. The particles are simply gravity fed into the transfer line by actuating an air cylinder, thus eliminating complex feed mechanisms. Operator control is completely remote, with pressure gages, level and flow monitors, and position sensors providing all necessary feedback. Flexibility in the routing of transfer lines eases restrictions on the location of other pieces of equipment. During several stages of refabrication, the material is pyrophoric, requiring inert atmosphere protection to prevent rapid oxidation and degradation. Conveying inside a closed pipeline with argon permits us to maintain a high-purity inert atmosphere. A closed system also eliminates dusting problems and

the release of radioactive contamination. To briefly describe HTGR fuel refabrication,² the process begins by loading uranium from a uranyl nitrate solution onto weak-acid resin beads in an ion exchange process. The loaded resin is then dried and carbonized at $\sim 800^{\circ}\text{C}$ to drive off resin volatiles, leaving behind UO_2 in a carbon matrix. The particles are then transferred to a second furnace where the UO_2 is partially converted to UC_2 at $\sim 1700^{\circ}\text{C}$ to improve the fuel's irradiation performance.³ Carbon and SiC coatings are then deposited on the particles. The function of the coatings is to retain fission products.

A composite x radiograph⁴ of the Triso⁵ design fissile particle is shown in Fig. 1. Each coating layer is designed for a specific purpose and must have certain specified properties. The innermost or "buffer" coating is composed of low-density pyrolytic carbon. The buffer provides void space for the accumulation of fission gases and shields the other layers from recoiling fission fragments. The next layer is known as a low-temperature isotropic (LTI) coating. The carbon is deposited at low temperatures compared with the temperatures of certain other processes, and the carbon must be crystallographically isotropic to avoid excessive shrinkage during irradiation. The LTI has a higher density than that of the buffer coating, and it acts as a pressure vessel to retain fission gases. This is the final coating for Biso design particles. The third layer applied to the Triso design fissile particle consists of high-density SiC, which acts as a diffusion barrier to certain metallic fission products. The final coating applied in the Triso design is an outer LTI, which enhances bonding with the carbonaceous matrix when the particles are formed into rods. The nominal characteristics for Biso and Triso design particles are presented in Table 1. Fissile and fertile fuel particles are blended and formed into fuel rods by a matrix-intrusion method. The rods are then loaded into holes in graphite elements, which are then carbonized and annealed at 1800°C . This scheme is illustrated in Fig. 2. Approximately 24,000 particles are contained in each fuel rod; each of the 4000 graphite elements in a 3700-MW(Th) HTGR core would contain 1500 fuel rods.



BUFFER
INNER LTI
SiC
OUTER LTI

Fig. 1. Multiple Pyrocarbon and Silicon Carbide Coatings Ensure Fission Product Retention in Triso Design Fuel Particles.

Table 1. Nominal Dimensions and Densities of the Triso- and Biso-Coated HTGR Recycle Fuel Particles

	Coating Thickness (μm)	Coating Density (g/cm^3)	Particle Diameter (μm)	Particle Density (g/cm^3)
<u>Fissile (Triso)</u>				
UO ₂ -UC ₂ kernel			400	3.2
Buffer	50	1.1	500	2.2
Inner LTI	35	1.9	570	2.1
SiC	30	3.2	630	2.4
Outer LTI	35	1.9	700	2.3
<u>Fertile (Biso)</u>				
ThO ₂ kernel			500	10.0
Buffer	85	1.1	670	4.8
LTI	75	1.9	820	3.5

In order to ensure satisfactory performance of the fuel, a particle batch might be weighed and sampled after carbonization and conversion as well as after each coating application. This scheme is shown in Fig. 3. Inside the furnace, the particles are contained within a crucible, which has a porous bottom.⁶ The particle batch is poured onto a vibrating screen, which removes soot balls and carbon flakes formed in the furnace during the coating operation. The particles are collected in a transfer hopper and pneumatically conveyed to a collection hopper atop the weigher and sampler. After these operations, the batch is returned to the coating furnace for further coating applications, or transferred to the fuel rod fabrication machine after the outer LTI has been applied.

A considerable amount of material handling is necessary during refabrication. Since fuel material must meet stringent quality assurance specifications before being qualified for reactor use, the effects of material handling must be minimized. One fuel parameter of particular concern is the number of defective particles (i.e., the fraction of particles within the batch having coatings that are chipped, cracked,

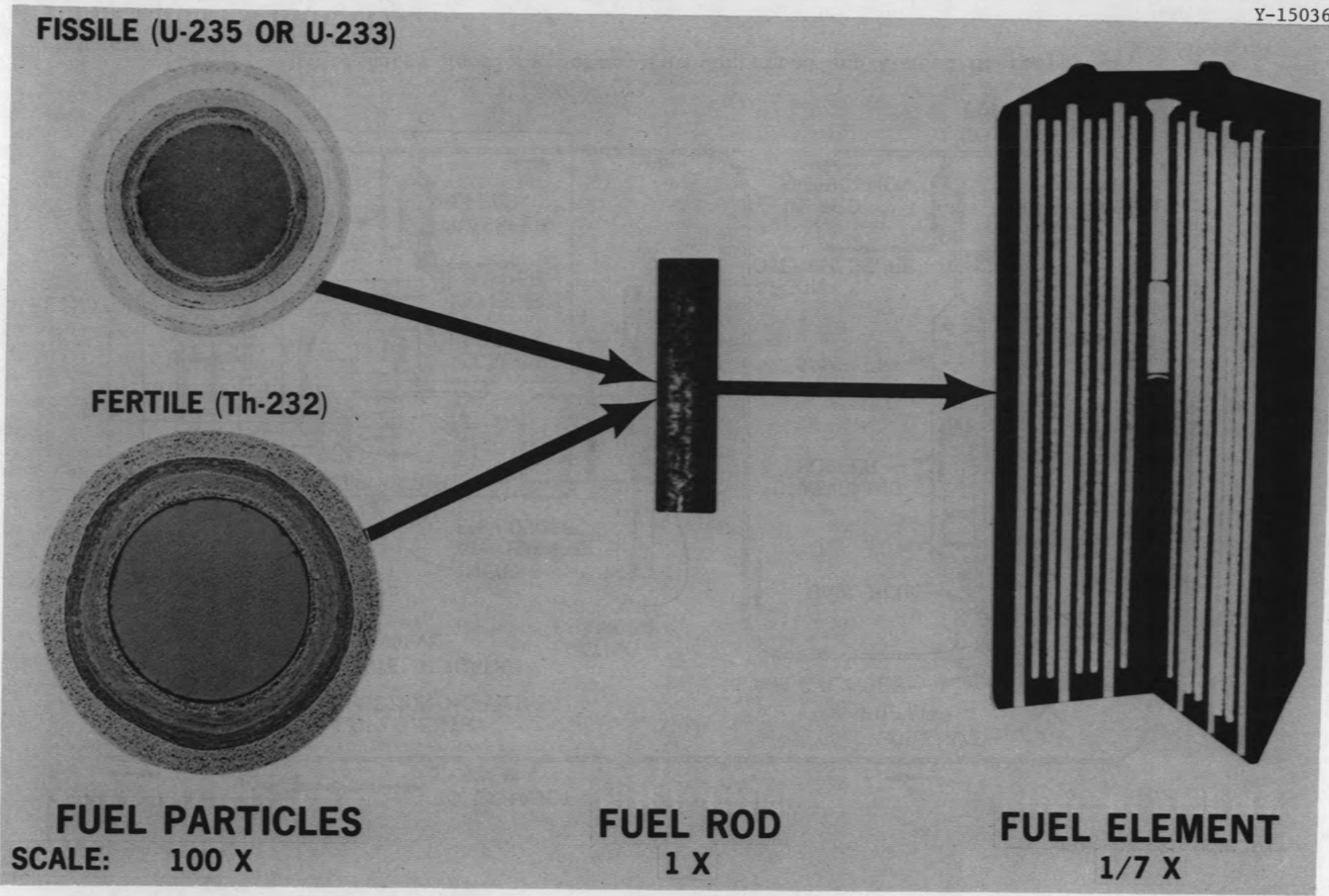


Fig. 2. HTGR Fuel Components.

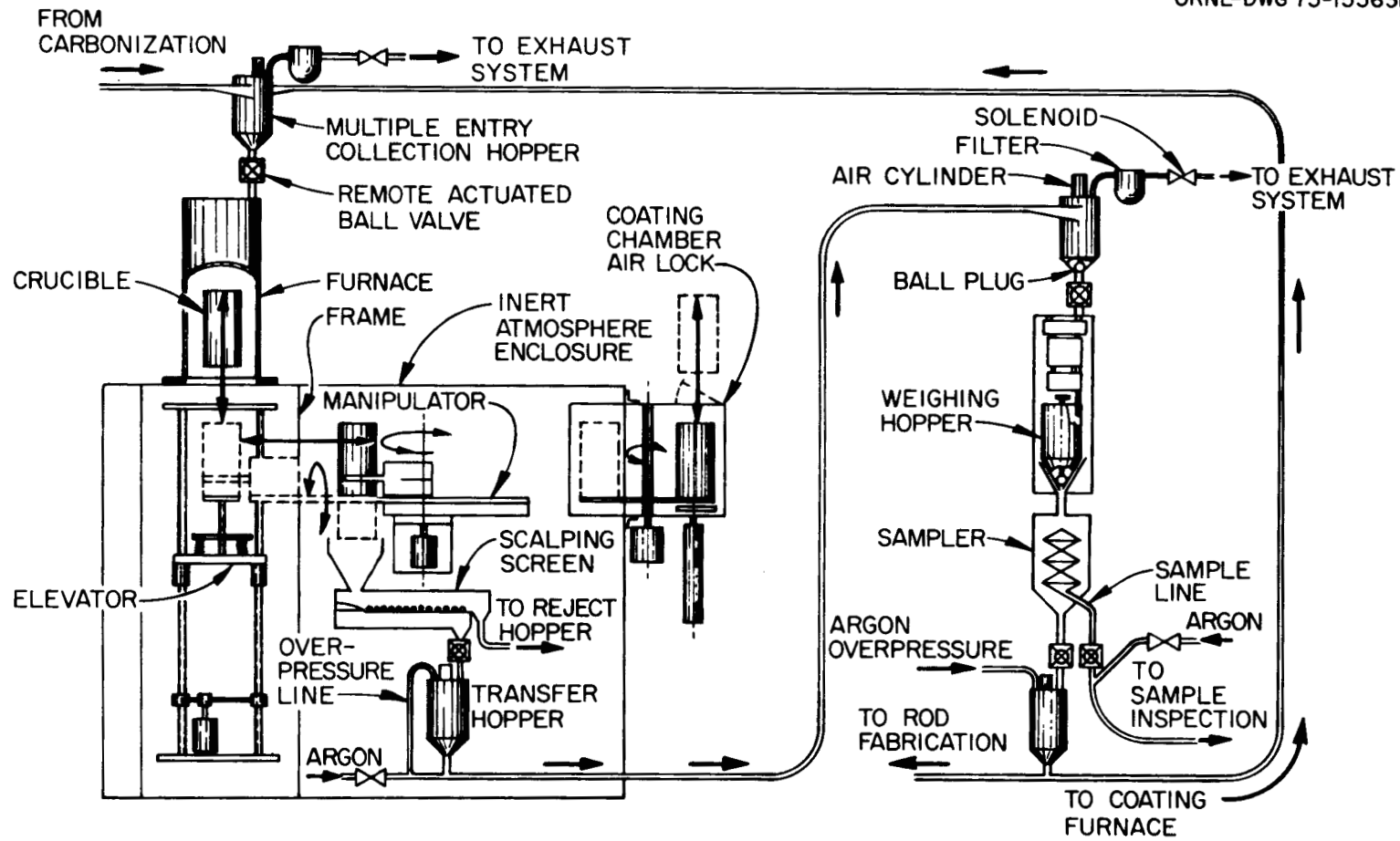


Fig. 3. Remote Batch Handling Scheme for Converted and Coated Microspheres.

or permeable to fission gases). Defective particles would release fission products into the reactor's coolant stream. In order to reduce this release to an allowable level, a particle failure fraction of less than 10^{-3} , or 0.1%, has been tentatively established as the specified limit for the entire refabrication process.

Since some breakage will inevitably occur during the various process steps, the pneumatic transfer system must be designed to minimize its contribution to particle breakage. This requires careful design of transfer components and necessitates conveying of the material at the lowest possible velocities. All components coming into contact with the particles must be free of ledges and cracks that could trap or damage the particles or their coatings. Since particles at different stages of refabrication will pass through the same equipment, those retained from one pass may be picked up in a subsequent pass, resulting in particles deficient in one or more coatings. These are also considered defective particles, since without the required number of coatings their probability of failure in a reactor increases.

TEST LOOP DESIGN

To determine the feasibility of pneumatic conveying for this application, a test loop was designed and constructed to provide general operating data on particle transfer characteristics as well as wear and breakage, from which the behavior of any system design configuration could be predicted.

Two 30-m (100-ft), 12.6-mm-ID (1/2-in.) transfer lines were constructed, one using polyethylene to obtain velocity data and the other using 15.9-mm-OD (5/8-in.) type 304 stainless steel tubing. Each line provided one 4.6-m (15-ft) and two 9.1-m (30-ft) horizontal runs and a 3.1-m (10-ft) vertical rise, incorporating five 90° bends, as illustrated in Fig. 4. An interchangeable 90° bend between pressure taps 8 and 9 permitted data acquisition for bend radii of 0.15 to 1.8 m (0.5–6 ft). The receiving hopper was located above the transfer hopper, and recirculation of a batch was accomplished

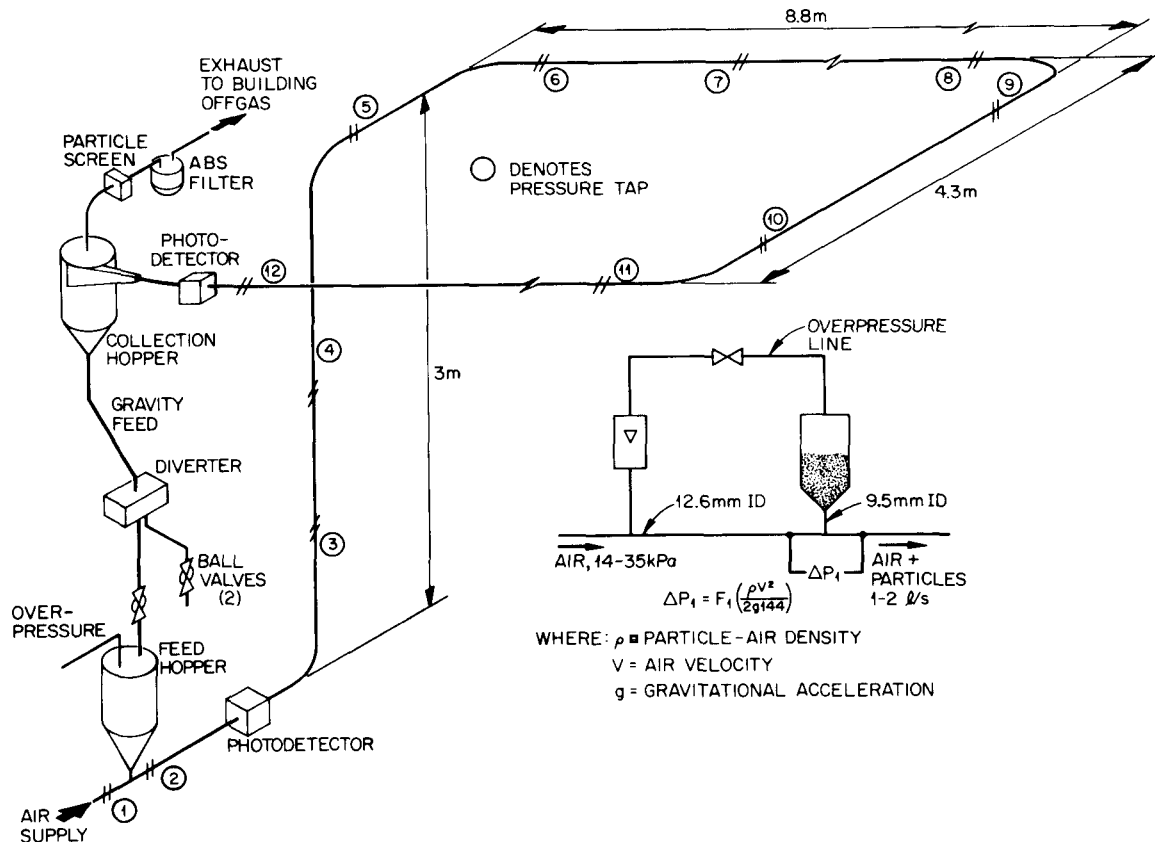


Fig. 4. Pneumatic Transfer Test Loop for Determination of System Operating Parameters.

by gravity feed through a diverter valve. Both hoppers were 127-mm-diam (5-in.) cylinders ~0.46 m (18 in.) in length with a 45° funnel-shaped outlet. The collection hopper was fabricated with a tangential inlet whose opposing tapers guide the particles toward the inner wall of the hopper by gradually changing from a circular to a thin rectangular cross section to reduce the severity of particle/wall collisions.

The system parameters monitored were air velocity, particle velocity, particle feed rates, density of the air-particle mixture in the line, and pressure drops during vertical and horizontal conveying. Airflow was measured at the exhaust port using a rotameter, while particle velocities were calculated from data obtained using photoelectric sensors. A holder was designed and fabricated that clamped onto the translucent polyethylene tubing,

positioning the sensor 180° from a small light source. Output from the detectors was fed to a recorder, the voltage of the signal being proportional to the amount of light reaching the detector. The sensitivity of the phototransistors was sufficient to detect small groups of particles passing through the line. Using two detectors and a high-speed recorder, average particle velocities through any segment could be calculated knowing the distance between the detectors. Since the photodetectors could not be used directly on the stainless steel test loop, 152-mm (6-in.) lengths of polyethylene tubing were inserted in line with the steel tubing, one at the beginning and one at the end of the 30-mm (100-ft) run. This permitted use of the detectors to provide data for calculating average particle velocities as well as the densities of the air-particle mixtures as discussed in the section on transfer characteristics.

Pressure drops in both systems were measured with pressure gages at various points using modified tubing unions, each consisting of a 73-mm (3-in.) length of copper tubing welded into a 6-mm-diam (1/4-in.) hole tapped into the union. A piece of fine wire mesh was placed inside the tube to prevent particles from entering, and a normally closed, quick disconnect fitting capped the copper tubing, thus permitting a number of pressure readings to be taken during each run using a single pressure gage.

The system was supplied with a 690-kPa (100-psi), 6-mm-diam (1/4-in.) compressed air line regulated from 0 to 103 kPa (0-15 psi), which was sufficient to provide airflows up to $2.8 \times 10^{-3} \text{ m}^3/\text{s}$ (6 scfm), corresponding to linear airflows up to 22.8 m/s (75 ft/s), and internal pressures up to 55 kPa (8 psig) during transfer. The transfer line was tapped upstream from the feed hopper to provide overpressure inside the hopper in order to prevent backflow or "percolating" of the air into the hopper as the particles fed into the line. The particles entered the transfer line through a 9.5-mm-ID (3/8-in.) tube to a 9.5-mm (3/8-in.) tee fitting chamfered to provide a smooth transition to the 12.6-mm-ID (1/2-in.) transfer line. This created a venturi effect, causing a slight increase in the air velocity

and a decrease in the pressure in the particle pickup zone to aid particle feed and entrainment. With the pressure equalized, the particles essentially gravity-fed out of the cylindrical hopper when a plunger, which had provided a particle seal on the funnel portion of the hopper, was lifted by actuating an air cylinder. At the receiving end of the transfer line, the particles were collected tangentially in the receiving hopper to minimize breakage. The transfer air was exhausted out the top of the hopper through a fine mesh screen and bell jar-type filter.

Commercial tube couplings were bored out to permit a single tube-to-tube interface. Chamfering of the tubing ends to permit smooth particle flow and to minimize breakage was abandoned since it created particle traps.

TRANSFER CHARACTERISTICS

A variety of particle types was transferred to provide data and operating experience with particles of 500- to 800- μm (0.020- to 0.032-in.) mean diameter having densities ranging from 1.7 to 4.4 g/cm^3 (100 to 275 lb/ft^3). In correlating the data, multiple regression analysis was utilized to evaluate the relative effects of these particle characteristics and other system variables on transfer behavior.

Flow through the transfer line for each of these particle types can be described as dilute phase conveying, wherein all of the particles remain entrained in the airstream and the density of the air-particle mixture in the line during transfer is fairly low, on the order of 16 to 32 kg/m^3 (1 to 2 lb/ft^3). Figure 5 illustrates variation in the average air-particle density with air velocity. As the velocity of the conveying air decreases, the amount of material in the line at any given time increases until saltation occurs. At saltation, the air velocity is insufficient to carry the particles along, and they become disentrained or "salt out" of the airstream, thus filling the horizontal sections and blocking the vertical sections. The "saltation velocity," or minimum transfer velocity, is higher for the more dense particles than for the lighter particles because of the higher load

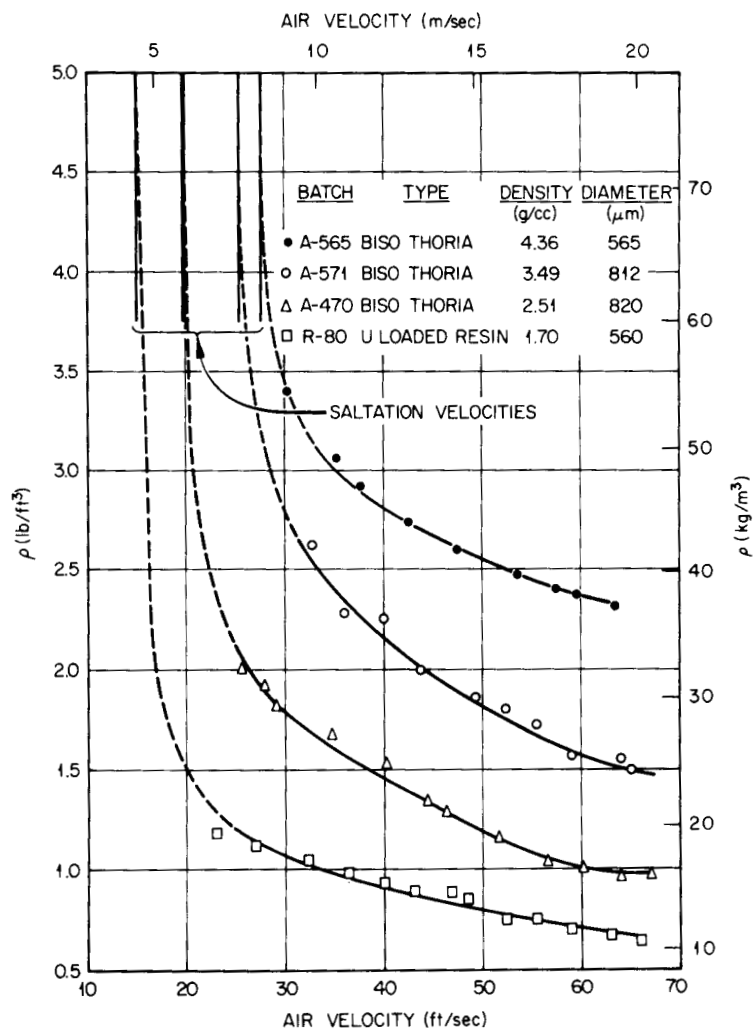


Fig. 5. Density of the Air-Particle Mixture vs Air Velocity for Pneumatic Conveying in 12.6-mm-ID (1/2-in.) Stainless Steel Tubing.

demand these particles place on the system (i.e., the higher density of the air-particle mixture). A purge pressure below ~103 kPa (15 psi) proved sufficient in reestablishing flow following a simulated loss of power shutdown, although it should be noted that this requirement is dependent on the number and length of vertical runs in a system (i.e., on the amount of material "available" for plugging a vertical rise). Horizontal lines are less prone to blockage because as the material disentrains, the cross-sectional area effectively decreases, and the air velocity is artificially increased, resulting in two-phase flow.

Average air-particle densities (ρ) were calculated using the known mass of the batch (M) and the time required for transfer according to the equation

$$\rho = (t_1/t_2)(M/v) , \quad (1)$$

where t_1/t_2 is the ratio of the time required for particles to travel between two detectors (t_1) to the total time required for the entire batch to pass the second detector (t_2). This ratio times the mass of the batch gives the average amount of material in the line during transfer. (The weight of the air in the line is negligible and was not included.) The final term (v) is the volume of the line between the two detectors. The average air-particle density is directly proportional to the feed rate and inversely proportional to the particle velocity. Increasing the air velocity decreases the particle's residence time in the line without appreciably increasing the feed rate, resulting in lower air-particle densities.

Figure 6 illustrates particle slip — the difference between air velocity and average particle velocity — for four particle types. The particle types depicted in Fig. 6 are (from top to bottom) the uranium-loaded resin, Biso-coated loaded resin, SiC-coated fissile particles, and Biso-coated thoria particles. The particles are moved along in the air stream by aerodynamic drag or "air friction." The amount of slip a particle experiences is dependent on the type of flow and the size, shape, texture, and weight of the particle, as well as on inter-particle and particle-wall interactions. Note the increase in particle slip as the particle density increases. The surface area of the particle increases at a rate proportional to the square of the diameter, while its volume is related to the cube of the diameter. As a result, particle mass increases at a faster rate than that of the area over which the conveying force may act. Consequently, larger particles of the same density exhibit increased particle slip, as do higher density particles of the same size. Particle velocities tend to drop sharply once the air velocity falls below 9.2 m/s (30 ft/s). Saltation then occurs at

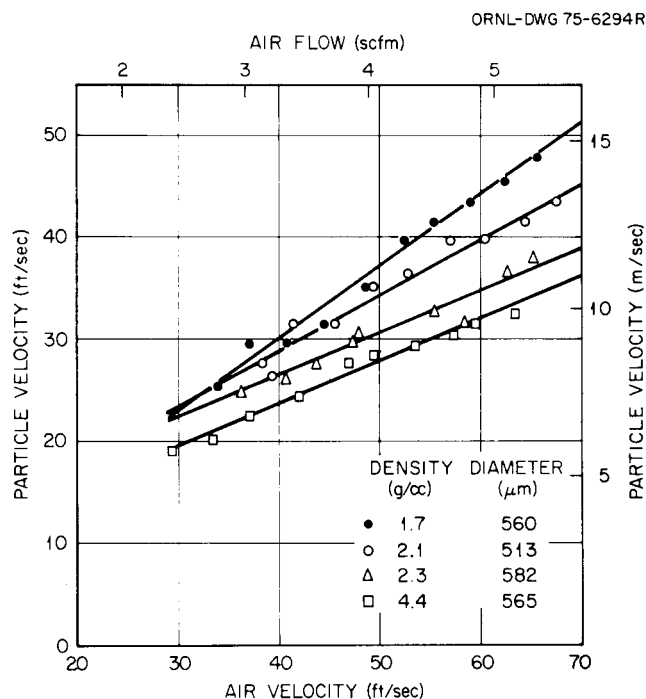


Fig. 6. Effect of Particle Density on Particle Slip During Pneumatic Transfer of Bare, Biso, and SiC-Coated Loaded Resin and Biso Thoria in Stainless Steel Tubing. To convert cfm to liters/s, multiply by 0.472.

air velocities of 4.6 to 7.6 m/s (15 to 25 ft/s), depending on particle type. The anticipated operating range is 3 to 4 scfm, corresponding to an average air velocity slightly less than 14 m/s (45 ft/s), which would be sufficient to keep each of the particle types entrained.

Of primary concern in pneumatic conveying is the pressure requirement of the system, not so much from the standpoint of maintaining a particular pressure drop (ΔP) as maintaining an adequate air flow rate, particularly since, for hot cell application, this system would operate from the building-regulated argon or air supply rather than employ blowers. Pressure drops along a line are additive and easily measured. The total pressure drop together with the air flow rate is necessary in determining system demand.

The largest single pressure drop in the system occurred at the point where the particles were fed into the line. In an effort to predict the behavior of any given particle type, an attempt was made

to empirically determine the acceleration factors for several particle types according to the method illustrated in Fig. 7. This equation in Fig. 7 represents the force required to accelerate the particles from rest expressed as a pressure differential.⁷ The figure also illustrates the 9.5-mm-OD (3/8-in.) valved overpressure line that bleeds air into the hopper, thus increasing the material flow rate linearly with increased flow through this line. The material flow rate increased 15 to 20% as flow through the overpressure line increased from 0 to 0.2 scfm.

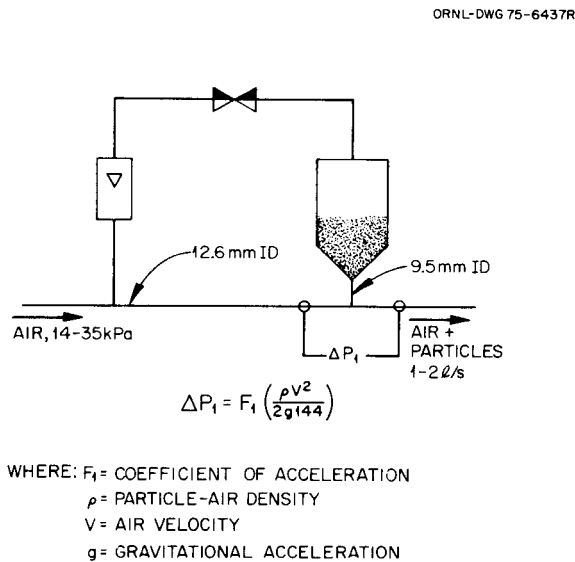


Fig. 7. Pressure Drop Caused by Acceleration of Particles from Rest.

Values of the coefficient of acceleration are plotted in Fig. 8 against the average velocity of the conveying air. The order and shape of the curves in this graph are the result of the $1/\rho$ and $1/V^2$ dependence of F_1 . As shown in Fig. 5, the density of the air-particle mixture, ρ , is highly dependent on particle density and is inversely proportional to the air velocity. These qualities dominate the curves in Fig. 8. This graph is useful in predicting pressure drops across the feed zone when used in conjunction with Fig. 5 to obtain densities of the air-particle mixtures. In this way, pressure drops can be calculated for any velocity of the conveying air.

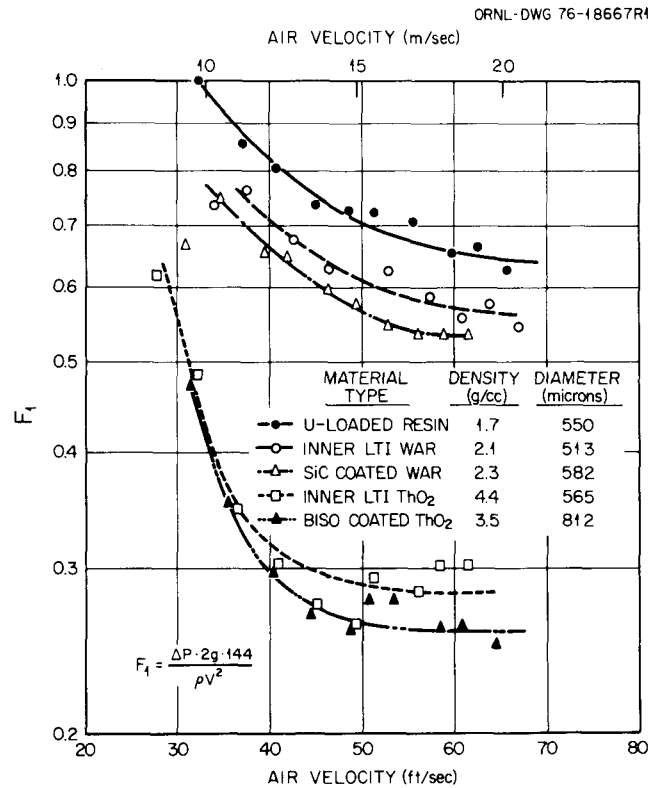


Fig. 8. Coefficient of Acceleration as a Function of Air Velocity for Several Particle Types in 12.6-mm-ID (1/2-in.) Stainless Steel Tubing.

In a similar manner, data on pressure drops in horizontal and vertical conveying were obtained for six different particle types ranging in diameter from 560 to 820 μm with densities of 1.7 to 4.4 g/cm^3 . Pressure drops in horizontal conveying were measured across points 7 and 8 in Fig. 4, corresponding to the last 3.7 m (12 ft) of a 7.6-m (25-ft) run. Due to practical limitations on the test loop design, the only section suitable for measuring pressure drops in vertical conveying was across points 3 and 4, consisting of a 0.76-m (2.5-ft) upward-only vertical section bounded by two 2-m (4-ft) radius bends. Since the bends had a large ID-to-radius ratio (~ 100), it was felt that any influence of the radial sections on conveying would be minimal.

In correlating the data, an attempt was made to formulate a mathematical equation for the pressure drop as a function of the mean particle diameter and density and the velocity of the conveying air.

A computer program⁸ utilizing multiple regression analysis was used to determine the coefficients in the equation and the correlation coefficient.

For the 60 data points on horizontal pneumatic conveying, the pressure drop over this range of particle sizes and densities was found to be best described by the equation

$$\Delta P_H = a_0 + a_1 V^2 + a_2 d + a_3 d^2 + a_4 \rho_P, \quad (2)$$

where

ΔP_H = pressure drop in horizontal pneumatic conveying through
12.6-mm-ID (1/2-in.) stainless steel tubing (kPa/m),

$$a_0 = 10.82,$$

$$a_1 = 2.78 \times 10^{-3},$$

V = velocity of the conveying air (m/s),

$$a_2 = 0.03549,$$

d = mean particle diameter (μm),

$$a_3 = -26.58 \times 10^{-6},$$

$$a_4 = -0.084, \text{ and}$$

ρ_P = mean particle density (g/cm^3).

This equation is plotted in Figs. A1, A2, and A3 in Appendix A, together with the data points used to generate these curves. A correlation coefficient of 94% was obtained with this equation, indicating very good agreement with the experimental data.

For the data on vertical conveying, the following equation was formulated, which had a 99% correlation coefficient:

$$\Delta P_V = b_0 + b_1 V^2 + b_2 d^2 + b_3 \rho_P, \quad (3)$$

where

ΔP_V = pressure drop in vertical pneumatic conveying through
12.6-mm-ID (1/2-in.) stainless steel tubing (kPa/m),

$$b_0 = -0.106,$$

$$b_1 = 0.00204,$$

V = average velocity of the conveying air (m/s),

$$b_2 = -0.28 \times 10^{-6},$$

d = mean particle diameter (μm),

$$b_3 = 0.645, \text{ and}$$

ρ_P = mean particle density (g/cm^3).

This equation is useful for predicting pressure drops for any material within the diameter and density range of the test batches. Results of observed data vs calculated curve are illustrated in Figs. A4, A5, and A6 in Appendix A. It should be noted that in both equations, with argon as the conveying medium, the actual pressure drops may be slightly higher than the predicted value due to the higher molecular weight (and density) of argon.

PRODUCT INTEGRITY

As part of the test loop evaluation, an attempt was made to quantitatively determine the degree of particle breakage that occurred during transfer. The procedure involved transferring a 2-kg batch of coated particles from the feed hopper to the collection hopper as many as 50 times at an average velocity of 6 to 7 m/s (20 to 23 ft/s). Samples were obtained by removing the batch from the system and riffling out an approximate 10-g sample. Defective coatings were detected by visual examination of the sample followed by chlorine leach analysis⁹ or mercury intrusion,¹⁰ depending on particle type. For Biso-coated particles, the samples were placed in a chlorine gas stream for 2 hr at 1500°C. The chlorine penetrated cracks in the coatings and reacted with the heavy metal in the kernel, forming a volatile chloride, which was driven off and condensed downstream. The defective fraction was then calculated from the amount of heavy metal in the condensate and the heavy metal content of the sample. Each SiC-coated particle sample was placed in a mercury pycnometer and pressurized to 103 MPa (15,000 psi), forcing mercury through any hairline cracks in the high-density SiC and into the voids in the porous pyrolytic carbon coatings. The particles were then removed from the mercury, cleaned of surface mercury, and x-radiographed.⁴ Microscopic examination of the radiograph slides permitted observation of mercury inside a defective SiC layer and thus allowed the number of particles having cracked SiC layers to be determined. Figure 9 is a portion of a radiograph slide showing a mercury-intruded SiC-coated particle. The mercury in the defective particle, like the heavy metal kernel, prevents the slide from being

Y-137827

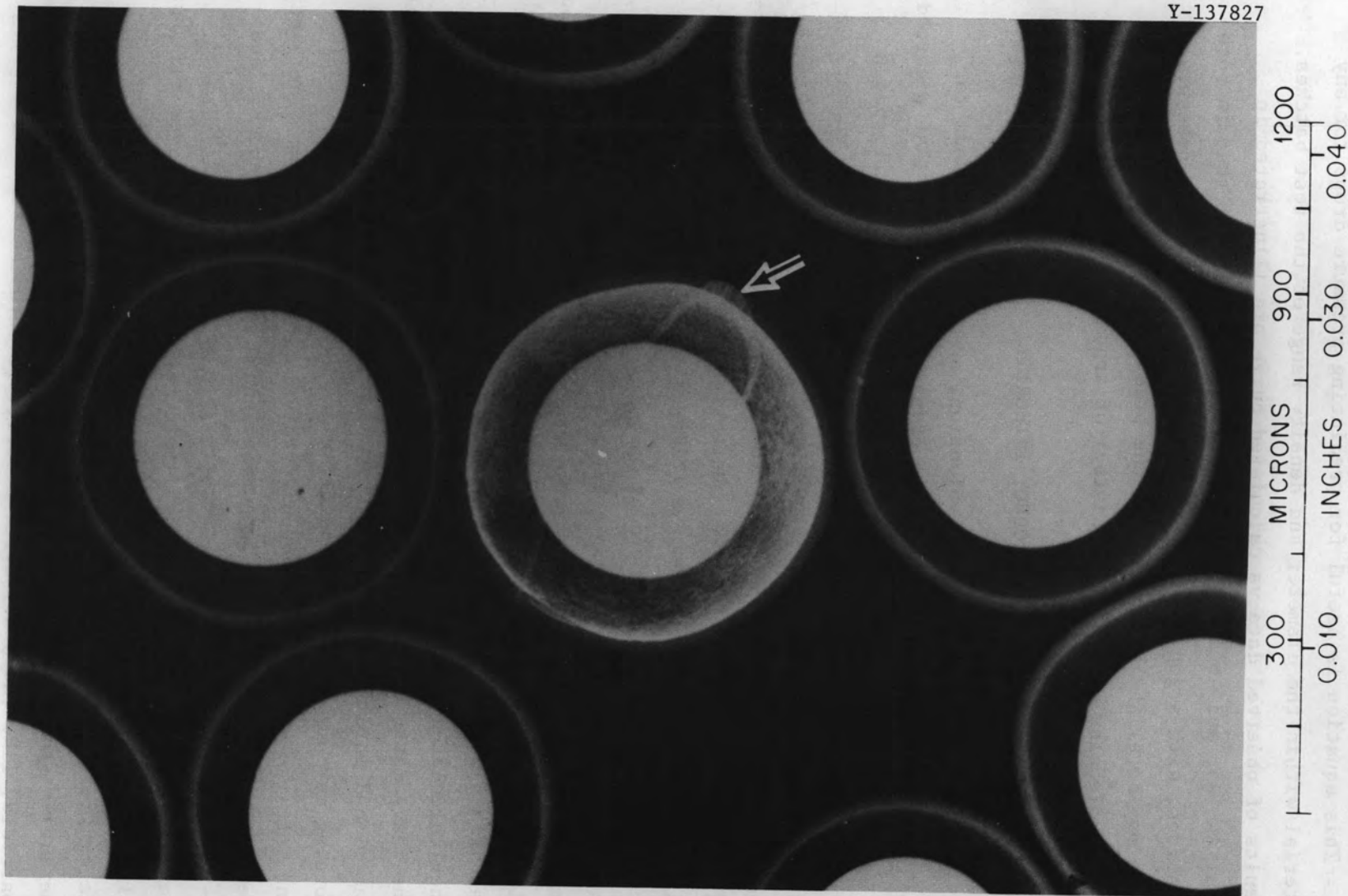


Fig. 9. Triso-Coated Fissile Particles Exposed to Mercury at 103 MPa (15,000 psi). Arrow indicates hairline crack in particle with defective SiC layer.

darkened by the x rays. Note the mercury deposited in the pores of the interior carbon coating as well as that remaining in the hairline crack around the circumference of the defective particle.

Each of the failure detection procedures is time consuming and costly to perform. As a consequence, the number of samples analyzed was limited to those necessary to indicate data trends for several different particle types. In addition to the uncertainties in the detection techniques themselves, the repeatability of the results was hampered by the low incidence (~1 defective particle per 10^4), the small sample size (10,000 to 30,000 particles), and the representability of each sample. In spite of these drawbacks, the data were adequate for determining trends in coating damage.

Initially, two Biso-coated thoria batches were chosen -- one consisting of large particles with thick coatings (reference fertile design) and a relatively high crushing strength¹¹ and the other of smaller particles with thinner coatings (reference fissile design) and a low crushing strength. The results of chlorine leach analyses are presented in Tables 2 and 3. The reference fertile design particles (A-571) performed extremely well, with no breakage indicated until the tenth transfer, after which a failure fraction of 1×10^{-4} was detected based on the average weight of thorium per particle. Performance of the fissile design batch was marginal. This was perhaps due to its unusually low crushing strength of 7.6 N (1.7 lb). Values for crushing strengths normally range from 9 to 30 N (2-7 lb), and a batch this weak could not meet fuel specifications and would be excluded from further refabrication.

Batches of other types of nonpyrophoric microspheres were transferred, including buffer-coated thoria and bare, uranium-loaded resin, with only minimal damage. Damage to the bare resin consisted mainly of the breaking off of small satellite spheres adhering to some of the larger particles, which were later removed by screening. Improved techniques for preparing the resin have eliminated these satellites prior to the uranium loading operation.

Table 2. Characteristics of Particles Used in Pneumatic Transfer Tests

Property	Batch A-571	Batch A-565
Buffer thickness, μm	85	51
Inner LTI thickness, μm	72	36
Diameter, μm	812	565
Density, g/cm^3	3.5	4.4
Crushing strength		
N	18.2	7.6
1b	4.1	1.7

Table 3. Chlorine Leach Analysis of Biso Thoria Samples Taken from a 1-kg Batch Pneumatically Transferred Through 30 m of 12.6-mm-ID Stainless Steel Tubing

Number of Transfers	Results for Batch A-571		Results for Batch A-565	
	Bare Kernels Visually Observed	Leached Kernels per 10^4	Bare Kernels Visually Observed	Leached Kernels per 10^4
0	0	0	0	0
1			0	0
2			0	0
3			0	4
4			1	3
5	0	0	1	6
6			5	16
7			0	3
8			1	7
9			1	10
10	2	1	1	11
15	0	0	3	28
20	1	1	0	26
25	4	4	0	56
30	1	3	4	64
35	4	5	7	82
40	5	7	1	87
45	3	3	6	228
50	3	3	2	100

Abrasive wear on the particle coatings ranged from 0.4 μm per transfer through the 100-ft stainless steel line for buffer-coated material to no wear detected for SiC-coated particles after 50 transfers. Some abrasion of the system did occur, as evidenced by iron contamination found in samples of a SiC-coated particle batch. Slight pitting occurred at the point where particles were fed into the line. No component failures attributable to material abrasion were experienced over the 2-year test period.

APPLICATION TO ENGINEERING-SCALE EQUIPMENT

This technology has been applied to the design, construction, and successful operation of a pneumatic conveying system supplying bare, uranium-loaded resin to a carbonization furnace and then transferring the pyrophoric carbonized kernels from the furnace to a glove box under inert atmosphere protection. This system is described in Appendix B. A second system is being installed for inter-laboratory transfer of the carbonized resin to a coating furnace. This will include two 30-m-long horizontal runs, a 5-m-long vacuum transfer run, and a 30-m-long particle vacuum transfer line, scheduled for operation in 1978.

SUMMARY

A low-pressure (0 to 100 kPa - 0 to 15 psig) pneumatic transfer system has been developed for conveying HTGR fuel microspheres for application in a remote refabrication facility. Particles in each of their nonpyrophoric stages, ranging in diameter from 500 to 800 μm with densities of 1.7 to 4.4 g/cm^3 , were pneumatically conveyed in batches of 1 to 2 kg between specially designed hoppers through 30 m of 12.6-mm-ID type 304 stainless steel tubing, at an average feed rate of approximately 1 kg/min. Minimum airflow requirements were determined for each particle type. Average particle velocities ranged from 5 to 25 m/s as measured with photoelectric sensors, while airflow ranged

from 1 to 3 liters/s (2 to 6 scfm). Phenomenological equations were successfully developed for pressure losses in vertical and horizontal conveying. Analyses of samples taken from batches transferred many times indicated minimal damage to the particles and their coatings.

Operation of the essential components was demonstrated, and auxiliary equipment such as diverter valves, bidirectional transfer and collection hoppers, particle level monitors, and particle flow meters are currently being developed.

ACKNOWLEDGMENTS

The authors wish to express their gratitude to C. L. Garrison for his operation and maintenance of the test loop throughout the project. The assistance of the following persons is also greatly appreciated: D. E. LaValle and F. L. Layton of the Analytical Chemistry Division for performing the sample analyses, M. G. Willey and J. L. Heck of Experimental Engineering for their design work on the hoppers and diverter valve, and B. J. Bolfig of the Instrumentation and Controls Division for designing the control panel, circuitry, and PLC interfacing for the carbonization furnace transfer system. The manuscript was reviewed by R. E. Helms, S. M. Tiegs, and W. J. Lackey. Technical editing was done by Debbie Stevens, and the manuscript was prepared for reproduction by Julia Bishop of the Metals and Ceramics Division Reports Office.

REFERENCES

1. J. D. Jenkins, S. R. McNeany, and J. E. Rushton, *Conceptual Design of the Special Nuclear Material Nondestructive Assay and Accountability System for the HTGR Fuel Refabrication Pilot Plant*, ORNL/TM-4917 (July 1975), pp. 27-58.
2. J. D. Sease and A. L. Lotts, *Development of Processes and Equipment for the Refabrication of HTGR Fuels*, ORNL/TM-5334 (June 1976).

3. F. J. Homan, T. B. Lindemer, E. L. Long, Jr., T. N. Tiegs, and R. L. Beatty, "Stoichiometric Effects on Performance of High-Temperature Gas-Cooled Reactor Fuels from the U-C-O System," *Nucl. Technol.* 35(2): 428-41 (September 1977).
4. R. W. McClung, *Studies in Contact Microradiography*, ORNL-3511 (October 1963).
5. W. O. Harms, "Carbon-Coated Carbide Particles for Nuclear Fuels," pp. 290-313 in *Modern Ceramics - Principles and Concepts*, ed. by J. E. Hove and W. C. Riley, Wiley, New York, 1965.
6. W. J. Lackey, D. P. Stinton, and J. D. Sease, "Improved Gas Distributor for Coating High-Temperature Gas-Cooled Reactor Fuel Particles," *Nucl. Technol.* 35(2): 227-37 (September 1977).
7. "Pneumatic Handling of Powdered Materials," *Engineering Equipment Users Association Handbook No. 15*, Constable and Company, Ltd., London, 1963.
8. A. J. Barr and J. H. Goodnight, *A User's Guide to the Statistical Analysis System*, Sparks Press, Raleigh, North Carolina, 1972.
9. D. E. LaValle, D. A. Costanzo, W. J. Lackey, and A. J. Caputo, *Determination of Defective Particle Fraction in HTGR Fuels*, ORNL/TM-5483 (November 1976).
10. D. M. Hewette II and W. R. Laing, "Determination of Defective SiC Layers in Coated Nuclear Fuel Particles," *Nucl. Technol.* 21(2): 149-50 (February 1974).
11. W. J. Lackey, D. P. Stinton, L. E. Davis, and R. L. Beatty, *Crushing Strength of HTGR Fuel Particles*, ORNL/TM-5132 (January 1976).

APPENDIX A

PRESSURE DROP VS AIR VELOCITY IN HORIZONTAL AND VERTICAL CONVEYING

PRESSURE DROP VS AIR VELOCITY IN HORIZONTAL AND VERTICAL CONVEYING

The following graphs were generated from the equations for pressure losses in vertical and horizontal pneumatic conveying in 12.6-mm-ID (1/2-in.) wall stainless steel tubing as described in the text. The equations were generated by a multiple regression analysis of over 50 data points, correlating pressure drop per unit length during conveying with particle characteristics such as mean particle diameter and density, and the flow rate of the conveying air.

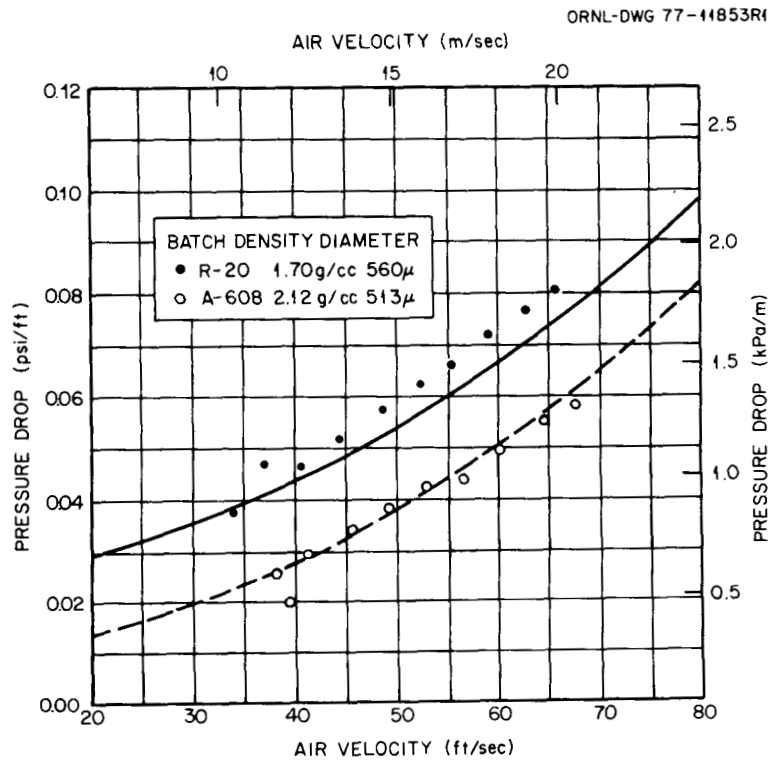


Fig. A1. Data and Least Squares Curve for Pressure Drop During Horizontal Pneumatic Conveying in 12.6-mm-ID (1/2-in.) Stainless Steel Tubing.

ORNL-DWG 77-11854R1

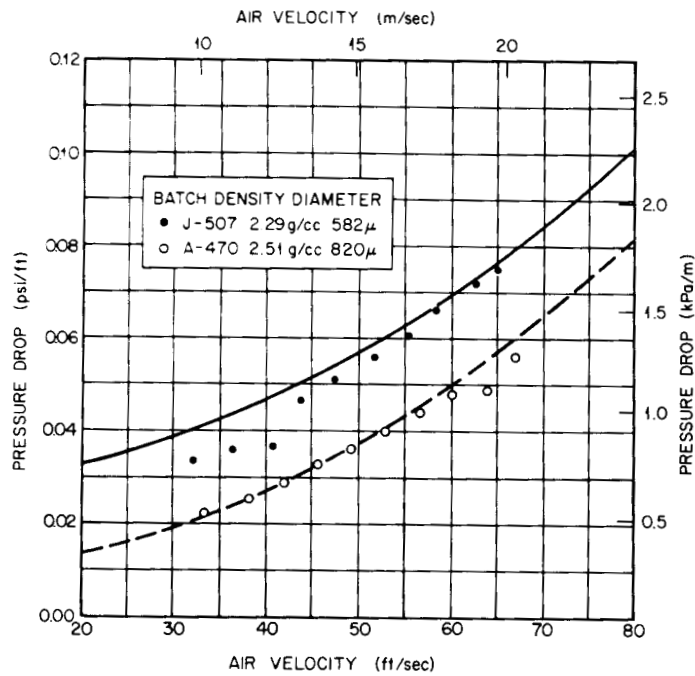


Fig. A2. Data and Least Squares Curve for Pressure Drop During Horizontal Pneumatic Conveying in 12.6-mm-ID (1/2-in.) Stainless Steel Tubing.

ORNL-DWG 76-20422R

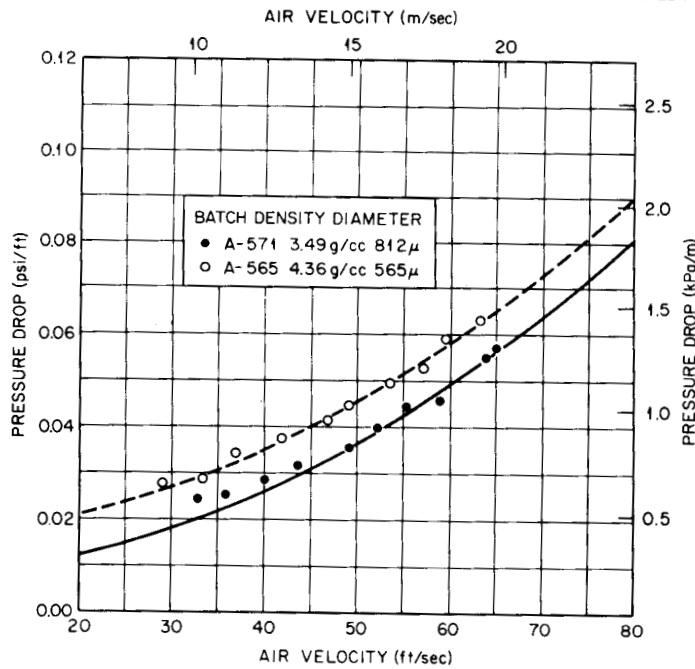


Fig. A3. Data and Least Squares Curve for Horizontal Conveying as a Function of Air Velocity, Particle Diameter, and Particle Density in 12.6-mm-ID (1/2-in.) Stainless Steel Tubing.

ORNL-DWG 77-12083R1

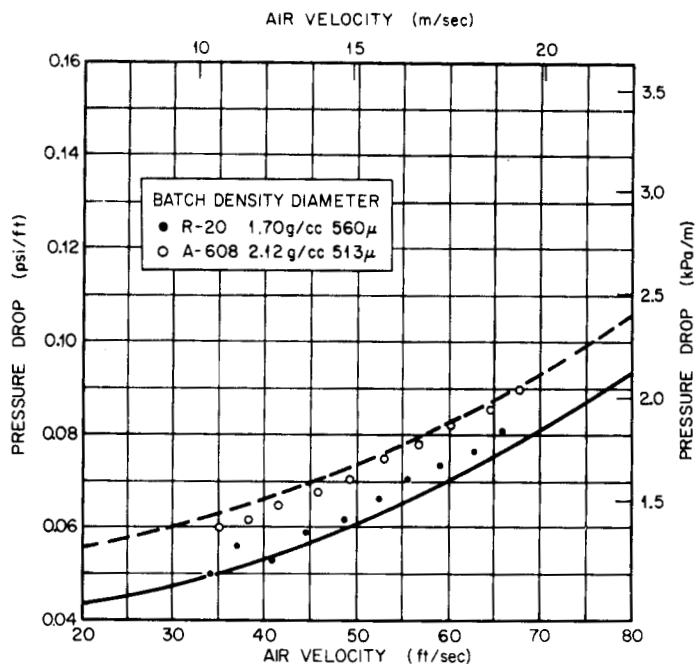


Fig. A4. Data and Least Squares Curve for Pressure Drop During Vertical Pneumatic Conveying in 12.6-mm-ID (1/2-in.) Stainless Steel Tubing.

ORNL-DWG 77-12084R1

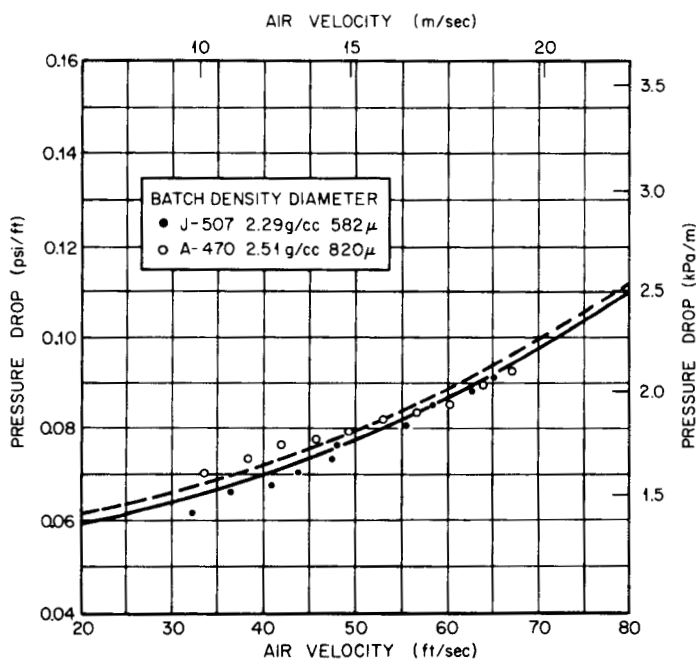


Fig. A5. Data and Least Squares Curve for Pressure Drop During Vertical Pneumatic Conveying in 12.6-mm-ID (1/2-in.) Stainless Steel Tubing.

ORNL-DWG 77-12085R1

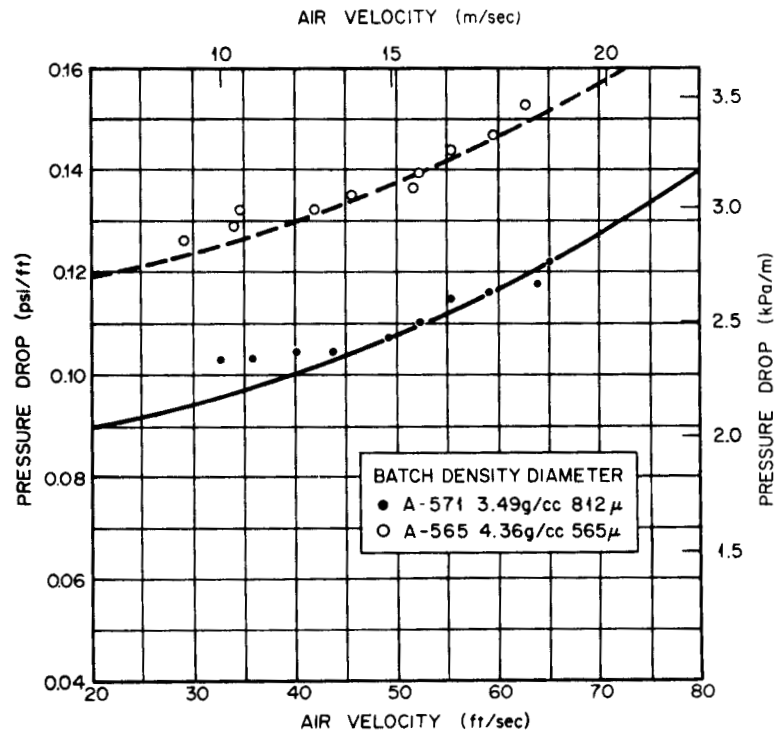


Fig. A6. Data and Least Squares Curve for Pressure Drop During Vertical Pneumatic Conveying in 12.6-mm-ID (1/2-in.) Stainless Steel Tubing.

APPENDIX B

RESIN CARBONIZATION FURNACE PNEUMATIC TRANSFER SYSTEM

RESIN CARBONIZATION FURNACE PNEUMATIC TRANSFER SYSTEM

This system has been designed to convey up to 8 kg of bare, uranium-loaded resin, which has a mean diameter of $\sim 500 \mu\text{m}$ and a particle density of 1.7 g/cm^3 . The resin is gravity fed from the laboratory container into the 24-cm-diam cylindrical transfer hopper shown in Fig. B1. A ball valve above the hopper, modified to eliminate particle entrapment, is closed to provide a airtight seal during transfer. An air cylinder-actuated spherical end plug acts as a particle seal on the funnel portion of the hopper. With the airflow set at 2 liters/s ($\sim 4 \text{ scfm}$), the plug is lifted and the particles flow through a 9.5-mm-diam orifice into the transfer line. At the point of entrainment, the bore of the transfer line has been reduced from 12.6 to 9.5-mm-diam, thus creating a slight venturi effect, which reduces the pressure and enhances particle feed. An over-pressure line is fed into the top of the hopper to equalize the pressure inside the hopper with that inside the line in order to prevent "percolating" of air back into the hopper as the particles are fed into the line. The particles travel a total of 2.5 m horizontally and 3 m vertically, with an estimated average velocity of 9 m/s and a feed rate of approximately 1 kg/min. They are received tangentially in a 24-cm-diam cylindrical collection hopper similar to the 13-cm-diam hoppers shown in Fig. B2. The opposing tapers of the entry tube guide the particles toward the hopper wall to minimize the severity of particle-wall and particle-particle collisions. The air is exhausted out the top of the hopper through a micromesh screen to a bell jar-type filter before being exhausted to the building off-gas system.

The particles are gravity fed into the furnace where they are carbonized in a fluidized bed at approximately 800°C , driving off hydrocarbons and leaving behind kernels consisting of UO_2 in a carbon matrix with a mean diameter of $400 \mu\text{m}$ and a density of 3.3 g/cm^3 . The nonpyrophoric particles are cooled to approximately 400°C and gravity fed out of the furnace through a remotely actuated modified ball valve into a transfer hopper by shutting off the fluidizing gas.

RESIN CARBONIZATION FURNACE FURNACE TRANSFER SYSTEM

Photo 3740-77

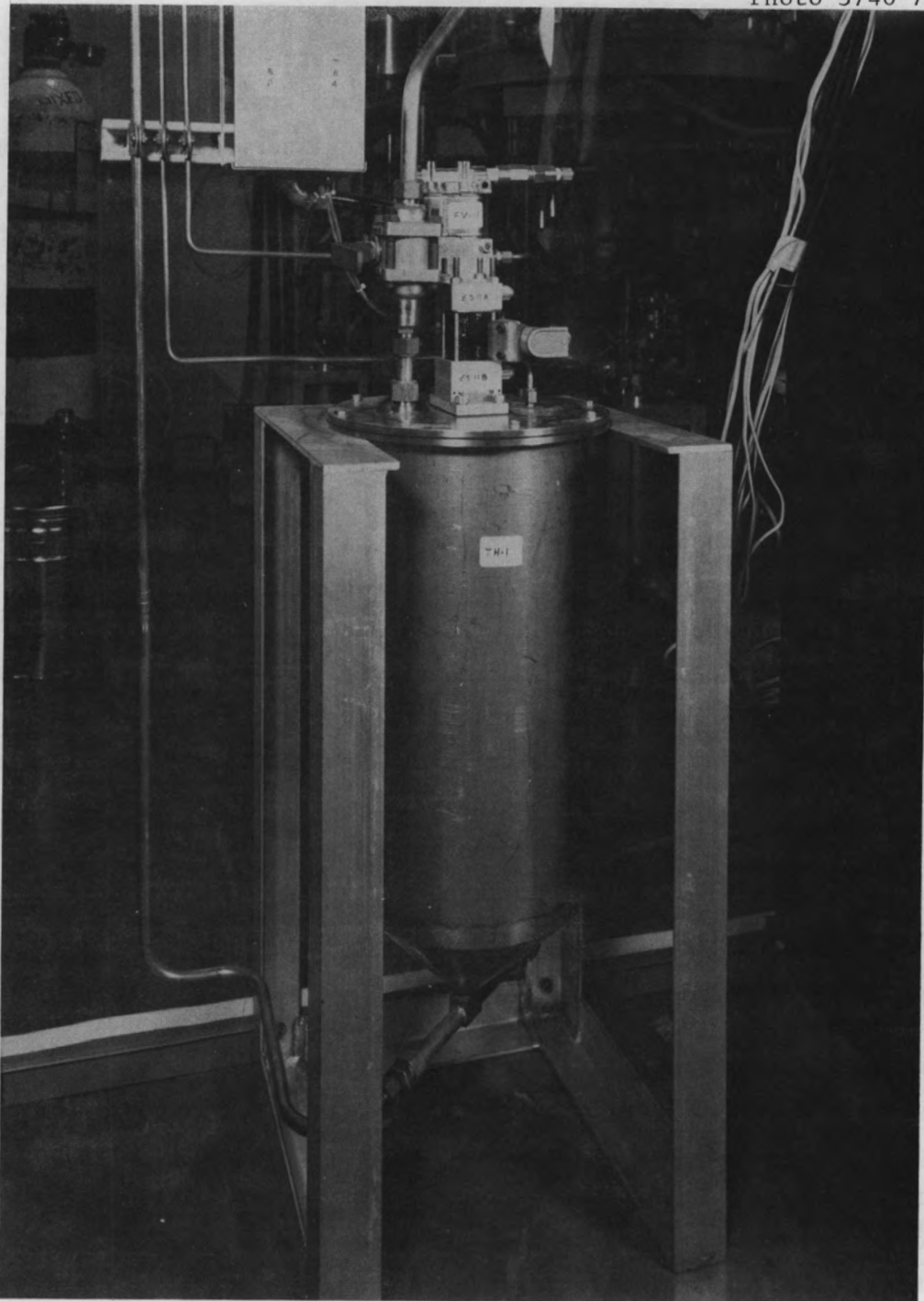


Fig. B1. Transfer Hopper, 23 cm (9 in.) in Diameter, Used for Conveying Bare Loaded Resin to the Carbonization Furnace.

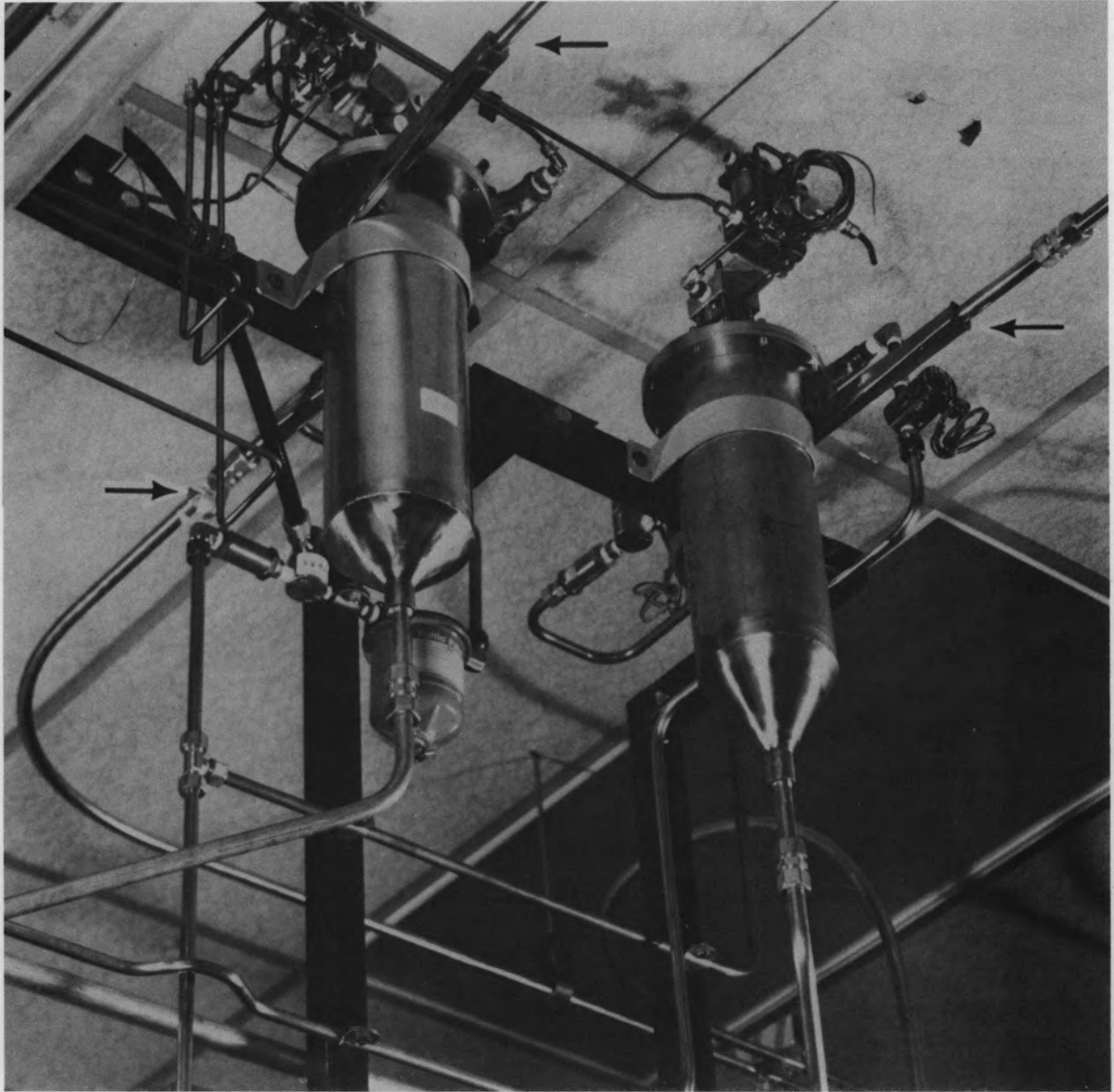


Fig. B2. Resin Carbonization Pneumatic Transfer System Collection Hoppers. Arrows indicate tangential inlets.

With argon as the conveying medium, the batch is pneumatically transferred to a collection hopper above an inert atmosphere glove box. The carbonized resin is then gravity fed into the glove box, where it is weighed and sampled.

The controls for this system are shown in Fig. B3. A graphic panel is used to display system status. The operator is relieved repetitive valve sequencing operations through the use of a programmable logic controller (PLC). This device minimizes the potential for operator error by performing routing valve sequences to effect transfer as well as by providing interlocks to prevent accidental spills or improper manual sequencing. Use of the video console shown in Fig. B4. permits manual override capabilities over PLC programming. This system has been in operation since September 1976.

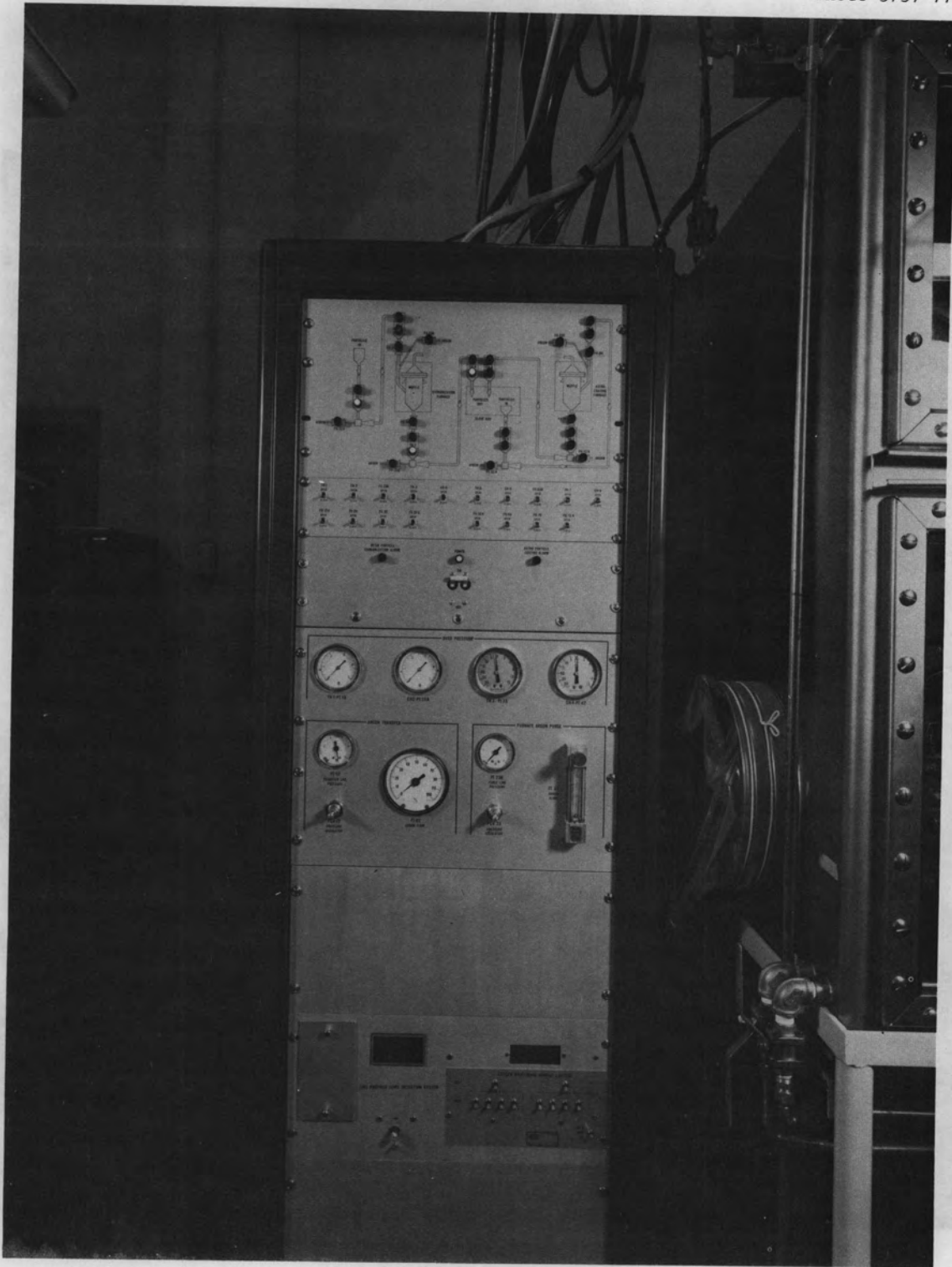


Fig. B3. Controls and Graphic Display Panel for Resin Carbonization Pneumatic Transfer System.

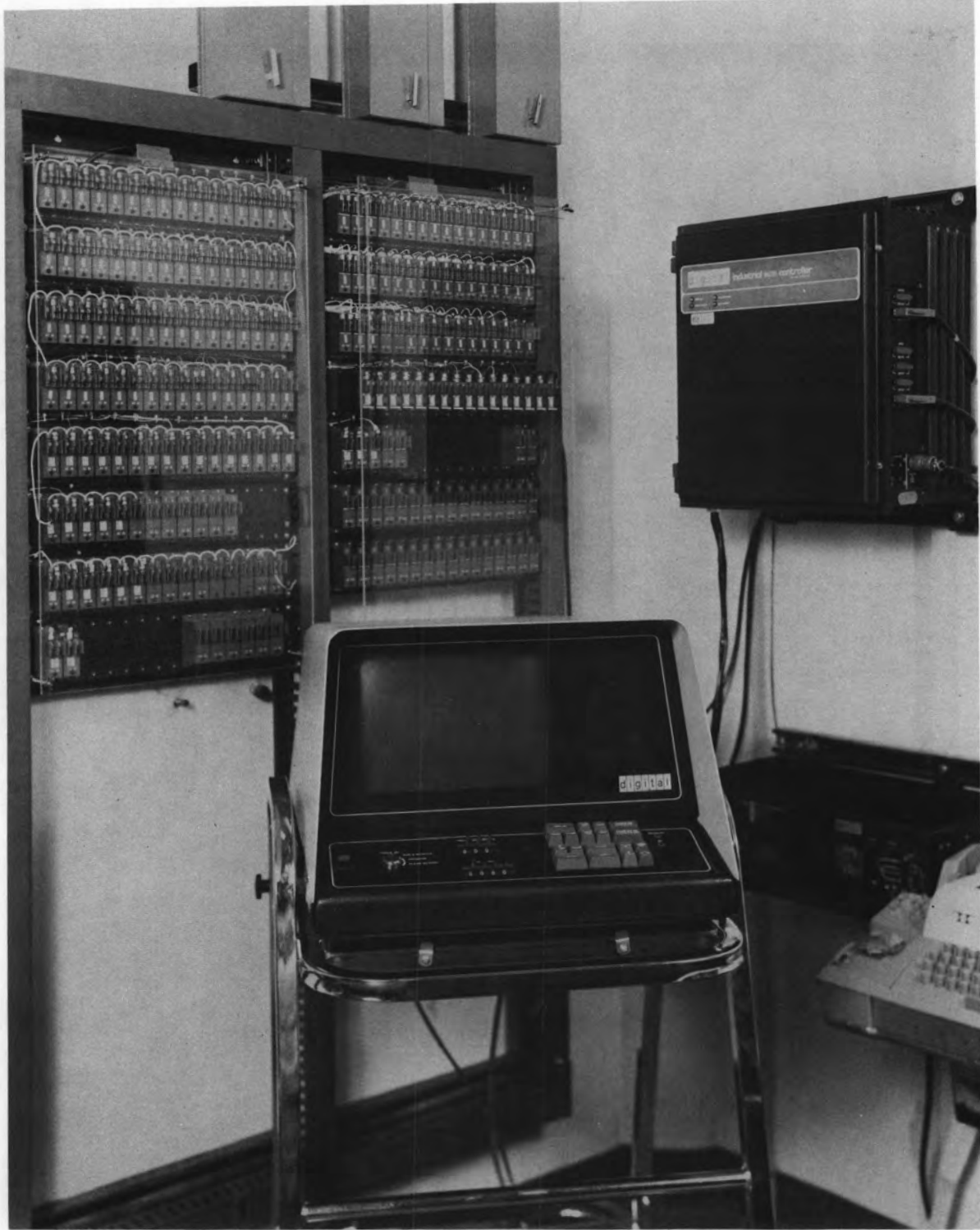


Fig. B4. Video Console and Input/Output Modules of the Programmable Logic Controller.

ORNL/TM-6169
 Distribution
 Category UC-77

INTERNAL DISTRIBUTION

- | | | | |
|--------|-------------------------------|--------|---------------------------------|
| 1-2. | Central Research Library | 51-56. | W. J. Lackey |
| 3. | Document Reference Section | 57. | E. L. Long, Jr. |
| 4-12. | Laboratory Records Department | 58-59. | A. L. Lotts |
| 13. | Laboratory Records, ORNL RC | 60-64. | J. E. Mack |
| 14. | ORNL Patent Office | 65. | M. M. Martin |
| 15. | R. K. Adams | 66. | S. R. McNeany |
| 16. | E. J. Allen | 67. | K. J. Notz |
| 17. | P. Angelini | 68. | A. R. Olsen |
| 18. | S. P. Baker | 69. | R. M. Peach |
| 19. | B. J. Baxter | 70. | H. Postma |
| 20. | R. J. Beaver | 71. | M. K. Preston |
| 21. | R. Blumberg | 72. | R. H. Rainey |
| 22. | B. J. Bolfig | 73. | D. P. Reid |
| 23. | R. J. Braatz | 74. | D. J. Richards |
| 24. | R. A. Bradley | 75. | H. D. Ringel |
| 25. | A. J. Caputo | 76. | T. F. Scanlan |
| 26. | J. A. Carpenter | 77. | J. E. Selle |
| 27. | D. A. Costanzo | 78. | W. D. Simpson |
| 28. | F. C. Davis | 79. | D. P. Stinton |
| 29. | J. P. Drago | 80. | R. R. Suchomel |
| 30. | R. G. Donnelly | 81. | V. J. Tennery |
| 31. | C. L. Garrison | 82. | B. A. Thiele |
| 32. | P. A. Haas | 83. | S. M. Tiegs |
| 33. | C. C. Haws | 84. | T. N. Tiegs |
| 34. | F. E. Harrington | 85. | D. B. Trauger |
| 35. | J. L. Heck | 86. | G. C. Wei |
| 36. | L. C. Hensley | 87. | J. R. Weir |
| 37. | R. E. Helms | 88. | M. G. Willey |
| 38-40. | M. R. Hill | 89. | J. W. Woods |
| 41. | R. M. Hill | 90. | R. W. Balluffi (consultant) |
| 42-46. | D. R. Johnson | 91. | P. M. Brister (consultant) |
| 47. | M. J. Kania | 92. | W. R. Hibbard, Jr. (consultant) |
| 48-50. | P. R. Kasten | 93. | N. E. Promisel (consultant) |

EXTERNAL DISTRIBUTION

- 94-95. DOE DIVISION OF REACTOR NUCLEAR RESEARCH AND APPLICATIONS,
 Washington, DC 20545
 Director
96. DOE IDAHO OPERATIONS OFFICE, P.O. Box 2108, Idaho Falls, ID 83401
 Barry Smith

EXTERNAL DISTRIBUTION (Continued)

97. DOE OFFICE OF PROGRAM MANAGEMENT, RESEARCH AND SPACE PROGRAMS,
P.O. Box 81325, San Diego, CA 92138
J. B. Radcliffe
98. DOE SAN FRANCISCO OPERATIONS OFFICE, 1333 Broadway, Wells Fargo
Building, Oakland, CA 94612
Manager
- 99-101. DOE OAK RIDGE OPERATIONS OFFICE, P.O. Box E, Oak Ridge, TN 37830
Director, Research and Technical Support Division
Director, Reactor Division
F. E. Dearing, Reactor Division
- 102-278. DOE TECHNICAL INFORMATION CENTER, P.O. Box 62, Oak Ridge, TN 37830
For distribution as shown in TID-4500 Distribution Category,
UC-77 (Gas-Cooled Reactor Technology)
- 279-286. DOE Exchange Agreements with Germany and Dragon Project